Published in final edited form as:
Biochim Biophys Acta. 2012 July ; 1817(7): 1053–1062. doi:10.1016/j.bbabio.2012.03.012.

Inter-monomer electron transfer is too slow to compete with monomeric turnover in bc_1 complex

Sangjin Hong[1,†,*], **Doreen Victoria**[1], and **Antony R. Crofts**[1,2,†,*]

[1]Departments of Biochemistry, University of Illinois at Urbana-Champaign, Urbana, IL 61801

[2]Center for Biophysics and Computational Biology, University of Illinois at Urbana-Champaign, Urbana, IL 61801

Abstract

The homodimeric bc_1 complexes are membrane proteins essential in respiration and photosynthesis. The ~11 Å distance between the two b_L-hemes of the dimer opens the possibility of electron transfer between them, but contradictory reports make such inter-monomer electron transfer controversial. We have constructed in *Rhodobacter sphaeroides* a heterodimeric expression system similar to those used before, in which the bc_1 complex can be mutated differentially in the two copies of cyt *b* to test for inter-monomer electron transfer, but found that genetic recombination by cross-over then occurs to produce wild-type homodimer. Selection pressure under photosynthetic growth always favored the homodimer over heterodimeric variants enforcing inter-monomer electron transfer, showing that the latter are not competitive. These results, together with kinetic analysis of myxothiazol titrations, demonstrate that inter-monomer electron transfer does not occur at rates competitive with monomeric turnover. We examine results from others groups interpreted as demonstrating rapid inter-monomer electron transfer, conclude that similar mechanisms are likely to be in play, and suggest that such claims might need to be re-examined.

1. Introduction

The cytochrome (cyt) bc_1 complexes are central components (as Complex III) of mitochondrial respiratory chains, in bacterial photosynthetic and respiratory chains, and in oxygenic photosynthesis (as cyt b_6f) [1–4]. The bc_1 complex operates through a Q-cycle mechanism that couples electron transfer from ubihydroquinone (QH_2) to cyt *c* to the generation of the proton gradient that drives ATP synthesis. The Q-cycle mechanism is well characterized, providing a parsimonious explanation for the observed behavior [5–9], but a role for the dimeric nature of the complex has been controversial [10–15]. The dimer interface between cyt *b* subunits brings the heme b_L centers within ~11 Å (for the electron transfer distance between conjugate systems) (Fig. 1), which might be expected to give rate constants much faster than the ms range of turnover (Table 1), leading to rapid electron transfer across the dimer interface. However, our previous work through titrations of QH_2

†To whom Correspondence should be addressed: Sangjin Hong or Antony R. Crofts, Department of Biochemistry, University of Illinois, 419 Roger Adams Lab, 600 S. Mathews Ave., Urbana, IL 61801, Phone: (217) 333-7407, Fax: (217) 244-6615, hong6345@illinois.edu; a-crofts@life.illinois.edu.
*These authors contributed equally to this work.

oxidation at the Q_o-site with myxothiazol had shown only linear titration curves diagnostic of monomeric function [12]. Recently, three groups have developed heterodimeric systems [16–18] allowing expression of two copies of the cyt *b* gene, and construction of strains differentially mutated so as to allow unambiguous tests of the hypothesis that electron transfer across the dimer interface occurs. All three groups have claimed to demonstrate an inter-monomer electron transfer between b_L hemes by measuring the rapid kinetics expected. One alternative electron transfer scheme, the half-of-sites mechanism [10, 19–21], requires such a transfer, but any scheme depending on a central role for such a process would require major revision of the Q-cycle, and such a paradigm change demands careful scrutiny. We have investigated the inter-monomer electron transfer using a heterodimeric system constructed for *R. sphaeroides* and were also able to demonstrate in strains mutated to enforce inter-monomer electron transfer the rapid kinetics that they observed. However, the rapid kinetics that they attributed to the inter-monomer reaction are, in our system, accounted for by cross-over recombination to generate a functional wild-type homodimer, and selection of the native sequence to allow survival under photosynthetic growth. From these results we conclude that, if inter-monomer electron transfer occurs, it is not rapid enough to allow effective competition with a monomeric function.

2. Materials and Methods

Plasmid pUC19 derivative containing *fbc* operon (pGB11BH6) was used as a template [22]. Mutant strains in cyt *b* at position 199 (Y199T, L, S, C, W, and insert Y199TY) were constructed by PCR-mediated site-directed mutagenesis [22–24]. For construction of heterodimeric expression system, linker and strep-tag sequences were inserted using PCR to generate pBST, pNT and pCT (Fig. S1). Site-directed mutagenesis at positions H111, G158 and H198 in cyt *b* was carried out using Transformer site-directed mutagenesis protocol. Two cyt *b* genes were fused using the *Not*I site introduced in the linker region, as described in [18]. All the mutations were verified by DNA sequencing. Growth in strain DH5α was used to amplify pUC19 derivatives. The 2.266 kb *Nsi*I/*Eco*RI restriction fragment of pNT was replaced with 2.272 kb *Nsi*I/*Eco*RI restriction fragment containing a factor Xa protease site and a strep-tag from pBST, generating pNTST. The 2.490 kb *Not*I/*Eco*RI restriction fragment from the pNTST was then ligated into 5.286 kb *Not*I/*Eco*RI restriction fragment of pCT to produce pBBST. Site-directed mutagenesis to generate heterodimeric constructions was performed in pNTST and pCT separately, followed by *Not*I/*Eco*RI digestion and ligation (Fig. S1). The oligonucleotide primers and *R. sphaeroides* strains used are listed in Tables S1 and 2.

The 5.133 kb *Hind*III/*Eco*RI restriction fragment containing the *fbcFB*$_1$*B*$_2$*C* operon was subcloned from pUC19 into pRK415, an expression vector, followed by transformation into *E. coli* S-17. The pRK415 derivative was then mobilized by conjugation from the S-17 into *R. sphaeroides* BC17, a strain in which the *fbc* operon had been deleted [24]. The site-directed mutations and the presence of strep-tag sequence at the C-terminus of fused cyt *b* in *R. sphaeroides* were confirmed by DNA sequencing after isolation of pRK415 and PCR amplification.

Chromatophores were prepared using the methods described earlier [25]. The computer-linked kinetic spectrophotometer was used for flash-induced kinetic spectrometric analysis as described previously [25]. The chromatophore concentration was adjusted to allow > 90 % saturation of the reaction centers by a single flash. Kinetics of redox changes of reaction center, cyt c_{total}, cyt c_2, cyt c_1, cyt b_H and cyt b_L were obtained by taking the differences in the kinetics of absorbance changes measured, respectively, at 542 nm, 551-542 nm, 550–554 nm, 552-548 nm, 561–569 nm, and 566-575-0.5(561–569) nm (with small additional

corrections for contributions from RC and cyt *c*), respectively. The measuring beam was turned off, and the reaction mixture in the cuvette was stirred between measurements.

3. Results

3.1 Myxothiazol titration of homodimeric complex to investigate inter-monomer electron transfer

We have previously demonstrated that titration curves for inhibition by myxothiazol of reduction of heme b_H via Q_o-site turnover in the presence of antimycin were linear, both in wild type and in strains mutated in the putative pathway for electron transfer across the dimer interface [12]. Tyr-199 (Y199) is the residue at the dimer interface in the most plausible pathway for electron transfer between the b_L hemes. All strains with single mutations at position 199 in cyt *b* (Y199T, L, S, C, W), and insert Y199TY, grew at normal rates under anaerobic photosynthetic conditions, and all showed turnover and redox properties for the bc_1 complex similar to wild-type. Properties for the strain with a threonine insert (Y199TY) were described earlier [23]. Similar linear titration curves are common in the literature for other Q_o-site inhibitors when the Q_o-site reaction is limiting [26–28]. Inter-monomer electron transfer would allow reduction of both b_H hemes through the Q_o-site of either monomer, so that strongly bowed titration curves would be expected. We suggested that the linear titrations observed were diagnostic of a monomeric mechanism [12].

We have extended these earlier studies to the titration behavior under controlled redox conditions after two flashes, and to the kinetic behavior of heme b_L. These experiments test the equilibria established for the Q_o-site reaction in the presence of antimycin. As shown in Fig. 2, although some small additional reduction of heme b_H occurred on the second flash, it was proportionally the same throughout the titration, and there was no indication that any additional *complement* of heme b_H became accessible to reduction through the uninhibited monomer; the titration after two flashes was still strictly linear (Fig. 2A). Instead, reduction of heme b_L occurred, and the relative amplitude showed the well-characterized equilibria expected from the monomeric Q-cycle [29] (Fig. 2B). Furthermore, the same behavior was seen in all strains mutated at Y199 in the most direct electron transfer path between the b_L hemes. If function of this pathway was critical to the ms kinetics of normal turnover, mutation might be expected to disrupt function, but strains Y199T, L, S, C, and W all showed close to wild-type kinetics. The kinetic behavior was similar even when the interface was modified by insertion of an extra threonine (Y199TY) to mimic the interface in the cyt b_6f complex, in which the configuration is substantially different. The behavior observed in all these experiments is consistent with monomeric function in the ms range.

3.2 Mutations in separate cyt b subunits of a heterodimeric complex to explore inter-monomer electron transfer

We have set up a heterodimeric expression system in *R. sphaeroides*. The general approach was similar to that used in *Rhodobacter capsulatus* [18], but the procedural details were adjusted to accommodate protocol differences in *R. sphaeroides* [22, 30] (Fig. S1 and Table S1). The *fbc* operon was modified so as to contain two copies of the gene for cyt *b* (*fbcB*$_1$ and *B*$_2$), separated by in-frame sequence encoding a linker span joining the two copies of cyt *b* in C- to N-terminal linkage, to give operon *fbcFB*$_1$*B*$_2$*C*. The linker span had the same sequence as in [18], and the downstream copy (*fbcB*$_2$) was modified so as to express a factor Xa cleavage site and a strep-tag at the C-terminal end. Site-directed mutagenesis was carried out on *fbcB*$_1$ and *B*$_2$ separately before joining with the linker. Using this strategy, we constructed heterodimeric variants in which different partial processes in the two copies of the protein were blocked by suitable mutagenesis. Mutation *b*G158W at Gly-158 of cyt *b* introduced a tryptophan side chain into the binding volume of the Q_o-site that blocked

access of substrate QH_2; mutation *b*H111N at His-111 of cyt *b* changed a ligand for heme b_H so as to prevent incorporation of the heme [30]; and mutation *b*H198N eliminated a ligand to heme b_L [30]. Following the nomenclature used in *R. capsulatus* [18], the heterodimeric construct with the wild-type sequence in both copies is indicated by B-B. Likewise, $_W$B-B^N indicates a construct with the G158W mutation in copy 1 and the H111N mutation in copy 2 of cyt *b*; ^N_WB−B, a construct with copy 1 inactivated by both mutations and copy 2 with wild-type sequence; and $_N$B-B^N, a construct with a heme b_L knocked out through mutation H198N in copy 1 and heme b_H knocked out in copy 2. We constructed a full set of combinations of these mutations (Table 2), including knockout mutations for heme b_L which have not been previously reported.

Table 2 shows strains that could grow photosynthetically at rates similar to wild-type, and those that failed to grow. Strains B-B, $_W$B-B^N, ^N_WB−B and other constructs previously reported [18], all showed similar behavior, all growing photosynthetically under anaerobic conditions. Strains ^{N}B-B^N, and $_W$B-B$_W$, both failed to grow photosynthetically, but grew under aerobic conditions. These results were in line with those previously reported [18]. The turn-over of the bc_1 complex in all the strains designed to express a heterodimeric complex were then assayed by comparing the kinetics of turnover of the photosynthetic chain through absorbance changes of the reaction center and the bc_1 complex [6, 25, 29, 31]. We followed reduction and oxidation of the *c*-hemes and *b*-hemes in the absence and presence of antimycin, and could demonstrate in strains B-B, $_W$B-B^N, and ^N_WB−B, the same general behavior as reported by [18], as seen in example traces for strain B-B and $_W$B-B^N in Fig. 3A. The traces of $_W$B-B^N showed rapid electron transfer kinetics similar to wild-type B-B. The spectra generated from such traces also showed involvement of all the Q-cycle redox centers with behaviors similar to the wild-type (Fig. 3B).

Surprisingly, strains $_N$B-B^N and ^{N}B-B$_N$ (not previously reported), in which a ligand for heme b_L (H198N) was mutated in one copy of cyt *b* and one for heme b_H (H111N) in the other copy, also grew photosynthetically. The electron transfer distance for the closest available path (the diagonal from heme b_L to b_H across the dimer interface) is ~23 Å (Fig. 1), giving a limiting value for the rate constant for QH_2 oxidation, k~10^{-1} s^{-1}, so growth would be expected only if some extraordinary reconfiguration of the complex had occurred, in which case some modification of behavior would have been expected. Nevertheless, the kinetics observed were similar to wild-type, excluding this unlikely event. We therefore checked the genetic complement encoding the bc_1 complex, using PCR amplification and DNA sequencing that would reveal the genotype encoding the wild-type behavior.

3.3 Homologous cross-over recombination and monomeric vs. inter-monomeric electron transfer

For all cultures used in kinetic experiments, the heterodimeric strains were checked for the presence of the expected mutations by sequence analysis after PCR amplification of the DNA encoding the heterodimeric *fbc* operon. The amplification was required after plasmid miniprep since the pRK415 plasmid harboring the *fbc* operon in *R. sphaeroides* is present in the cell in low copy-number. We used two sets of primers for sequencing of heterodimeric cyt *b* genes; one set that anneals specifically to the upstream sequence of the gene for cyt *b* and the linker sequence, and the other to the linker and strep-tag sequences. In all cases, sequence analysis showed in all the mutant strains the presence of the mutated sequence expected.

In order to check for the presence of intact heterodimeric *fbcFB*$_1$*B*$_2$*C* constructs in the mutant strains, we used a different set of primers that anneal to sequences upstream (in *fbcF*) and downstream (in *fbcC*) of the gene for cyt *b*which would allow us to distinguish by size

of PCR products, the heterodimeric *fbcFB*$_1$*B*$_2$*C* construct from any other forms of *fbc* operon (Fig. 4B). Interestingly, the pattern of amplified PCR products of the heterodimeric constructs from the cells used for preparation of chromatophores tested in kinetic experiments fell into two groups, one of which showed two major bands that correspond to the sizes of heterodimeric *fbcFB*$_1$*B*$_2$*C* and homodimeric *fbcFBC* and the other with only one major band at the same position on the gel as homodimeric *fbcFBC* (Fig. 4A) Sequence analysis showed that the bands with higher molecular weight (MW) retained the heterodimeric constructs with expected mutations whereas the bands with lower MW contained a homodimeric *fbc* operon with wild-type sequence. The sequencing of the bands also identified in both bands the strep-tag that was used for heterodimeric construction. Since the strep-tag was introduced into the heterodimeric construction specifically for this work, the presence of strep-tag in the bands with lower MW clearly indicated that the DNA encoding the homodimeric *bc*$_1$ did not come from an extraneous source, but was derived from the heterodimeric *fbcFB*$_1$*B*$_2$*C* construct.

4. Discussion

4.1 Kinetic analysis

The kinetics of the partial processes measured on turnover of the Q_o-site when the Q_i-site is blocked by antimycin, reflect the equilibrium constant of the bifurcated reaction, and equilibria in the high and low potential chains. The equilibrium constants are given by the redox potentials of the centers involved. For oxidation of QH_2 from the pool in the monomeric case, the overall equilibrium constant is given by

$K_{eq}=\exp(F/RT(E_L^{o'}+E_H^{o'}-2E_{Q/QH_2}^{o'}))$, where subscript *L* and *H* indicate acceptors in the low and high potential chains. The value of K_{eq} depends on the redox potentials of the acceptors available [5–7]. For the first QH_2 oxidized, the acceptors are heme b_H ($E^{o'}$ ~40 mV) and (predominantly) ISP_{ox} ($E^{o'}$ ~300 mV), and, with Q/QH_2 at $E^{o'}$ ~90 mV, K_{eq1} has a value of ~500. For the second QH_2, since the two more favorable acceptors have been consumed, the acceptors are heme b_L ($E^{o'}$ −90 mV) and (predominantly) heme c_1 ($E^{o'}$ 270 mV), and K_{eq2} has a value ~1. If inter-monomer electron transfer occurred, the equilibria would reflect the ability of one Q_o-site to deliver electrons to two equivalents of heme b_H, and this would be particularly obvious from kinetics measured near the midpoint of an inhibitor titration. These conditions are important because the second flash pumps up the redox potential in the high-potential chain, increasing the driving force for heme *b* reduction. The linear titration shows unambiguously that the fractional reduction of heme b_H is proportional to the fraction of active Q_o-sites remaining. Similarly, the pattern of behavior on two flashes is that expected from a monomeric mechanism. Both are inconsistent with inter-monomer electron transfer without introduction of additional hypotheses. It might be argued that the half-of-sites hypothesis [10, 16, 32] can account for the titration data; if only one monomer is active, all heme b_H would still undergo reduction. However, that would require two turnovers of the active Q_o-site, and fractional inhibition would then eliminate heme b_H reduction proportionately. To account for the monotonic curves observed [10, 16], the mechanism then requires that all steps, including inter-monomer electron transfer, must be at intrinsic rates much faster than the rate determining QH_2 oxidation. The observation that such rapid reduction of heme b_H could be observed in the presence of antimycin in heterodimeric strains mutated to enforce inter-monomer transfer [16] seemed to provide strong support for such a mechanism. The only missing component was then a plausible explanation for why the Q_o-site could function in only one of the monomers. In this context, the classical Q-cycle would have to be amplified by *ad hoc* accretions, and the natural interpretation of the kinetic behavior that seemed to support it so parsimoniously, would have to be extensively re-interpreted. Clearly, the evidence for inter-monomer electron transfer then needs careful examination before such a major change in paradigm becomes accepted.

It might be argued that the discrepancy between the ~10^6 s^{-1} rate constant calculated from distance (Table 1) and the minimal rate (~1 s^{-1}) suggested by the observed kinetics is so large as to discount any explanation. As noted in [12], there are several effects that might account for the difference. As argued by Shinkarev and Wraight [15], competition between alternative pathways to hemes b_H and b_L can explain part of the discrepancy (about 2-orders of magnitude). A more significant fraction would have to come from quantum mechanical effects [33–39]. The simple approximation from distance-dependence seems to work well in most cases [40–45], but use of the Hopfield approximation [46] in the Moser-Dutton approach [47] leads to loss of detailed balance, suggesting that the quantum mechanical adjustments are made in the wrong part of the equation [12, 48]. Winkler and Gray [49] have shown experimentally that electron transfer to the heme of cyt b_{562} through a direct path terminating at a liganding histidine can lead to rates lower than those expected from distance by factors ~10^3, and Prytkova et al. [39] explained this result using a quantum mechanical approach involving path-integrals which showed different contributions from interference effects in such direct pathways compared to edge-linked pathways. Hoffman et al. [50] have shown that electron transfer across a protein interface may be much slower than expected from distance. Other effects to be considered are local electrostatic fields, and distribution of electron or hole occupancies around the conjugate system of the heme acting as donor or acceptor; Walker [51–52] has examined the singly occupied molecular orbital of *b*-type hemes, and noted an asymmetrical distribution that would favor the intra-monomer case if it applied in the bc_1 complex. There are therefore realistic physical mechanisms that might be invoked to explain the slow rate observed.

4.2 A genetic mechanism accounts for the rapid kinetics observed

Cross-over by homologous recombination (Fig. 5A) is a well-characterized feature of genetics, ubiquitous in all realms of life [53–54], but was not addressed in [16, 18] and only minimally in [17]. Since this behavior provides an obvious mechanism for the results observed, we checked the sequence of the genetic complement encoding the bc_1 complex from *R. sphaeroides* cells at an early stage of photosynthetic growth in order to find any recombination intermediates. In the $^{N}_{W}B-B$ strain, we found two homodimeric constructs containing ^{N}B and B (wild-type) both with a strep-tag in the lower MW recombination product, which are the intermediates expected by a single cross-over recombination as suggested in the mechanism in Fig. 5A. We also checked for the complement encoding the bc_1 complex at different stages in the protocol used for construction of the mutant strains. As seen in Fig. 5B, both the heterodimeric construct, and homodimeric operon generated by recombination, were present even in the initial stages of the protocol. The heterodimeric *fbcFB*$_1$*B*$_2$*C* constructed in plasmids pUC19 and pRK415 in *Escherichia coli* strains DH5α and S-17 respectively, had been re-constructed to a homodimeric *fbcFBC*and both types of operon were maintained in the cells, although only the heterodimeric construct had been initially introduced into the strains. The *E. coli* DH5α and S-17 [55–56] are RecA-deficient strains. However, the substantial homology (~1.37 kb) of the two *fbcB* genes in tandem in the heterodimeric construct allowed *recA*-independent cross-over recombination [57–59], producing the recombinant homodimeric operon. Plasmid pRK415 is the vector used in conjugation from *E. coli* S-17 to *R. sphaeroides* so it seems possible that both types of operon were transferred to *R. sphaeroides* on conjugation. As noted in Materials and Methods, all plasmids encoding the bc_1 complex were expressed in the BC17 strain of *R. sphaeroides* with chromosomal deletion of the *fbc* operon, so that recombination reflects only plasmid events. Although we cannot know whether a particular cell contained one or both operons, the outcome on growth of the cultures was unambiguous. In all cultures, the *fbcFBC* operon for expression of a wild-type homodimeric bc_1 complex was the dominant DNA (Fig. 4A). In strains expressing at least one copy of a functional monomer in the heterodimer (B-B, ^{N}B-B, $_{W}$B-B and $^{N}_{W}B-B$), the heterodimeric construct was also

maintained on photosynthetic growth, as shown by the less prominent band. This shows that a monomeric function is sufficient to allow competitive expression. In contrast, in strains in which the heterodimeric construct encoded a complex with different crippling mutations in the two copies of cyt *b* ($_{W}$B-B^{N}, ^{N}B-B$_{W}$, $_{N}$B-B^{N} and ^{N}B-B$_{N}$), only the recombinant operon expressing a homodimeric complex with wild-type cyt *b* was maintained at significant levels. Although the recombinant homodimeric operon contributed the only significant PCR product in these strains and the heterodimeric construct was not seen at a level we could detect on gels (Fig. 4A), the latter was still present at a level that could provide a template for PCR amplification for sequence analysis when the primers annealing only to the heterodimeric constructs were used (see above). In support of the hypothesis of cross-over recombination, in strains in which both copies of cyt *b* had the same crippling mutation (^{N}B-B^{N} and $_{W}$B-B$_{W}$), no photosynthetic growth was observed, and no re-construction of the wild-type homodimeric expression system was detected.

Perhaps the most interesting secondary observation was the difference between levels of the two types of operon in the $_{W}$B-B^{N} strain when grown under aerobic or anaerobic conditions in *R. sphaeroides* (Fig. 5B). Under aerobic conditions, *R. sphaeroides* can grow without a functional bc_1 complex by using ubiquinol oxidase, whereas under anaerobic conditions, photosynthetic growth requires a functional bc_1 complex. When grown under aerobic conditions, cultures of the $_{W}$B-B^{N} strain maintained both the heterodimeric *fbcFB*$_1$*B*$_2$*C* and the homodimeric *fbcFBC* constructs. However, when grown photosynthetically, the cultures maintained only the homodimeric construct expressing the wild-type bc_1 complex at levels detectable on gels after unbiased PCR amplification.

From the above, it seems clear that we have observed a pretty example of micro-evolution, driven by the need for a functional bc_1 complex. Cells with heterodimeric complexes enforcing inter-monomer electron transfer do not compete effectively with those containing wild-type homodimeric complexes resulting from cross-over recombination. On the other hand, cells expressing heterodimeric complexes with at least one functional monomer are sufficiently competitive as to allow the culture to maintain both expression systems. The obvious conclusion is that inter-monomer electron transfer does not occur at rates competitive with monomeric function.

Although our results pertain only to the particular expression system constructed in *R. sphaeroides* and our conclusions have a definitive status only in that context, the mechanism of cross-over by homologous recombination is ubiquitous. Whenever two genes with homologous sequence spans are present in the same cell, recombination might be expected [54, 57–60]. Apart from a brief note on reversion frequencies in [17], neither the question of recombination nor steps taken to ameliorate it were mentioned in the earlier papers [16–18]. However, three papers [61–63] containing further details have now become available, which make it abundantly clear that the two labs working with *R. capsulatus* experienced difficulties similar to those we reported. The critical areas now to be addressed are the paradigm-changing claims made in the three earlier papers, the problems exposed in this paper, the new information from the three more recent papers, and any reinterpretation of the earlier claims needed to accommodate the new data.

In electronic circuits, the bus bar feeds the active components without significant impediment through a high-conductivity path which carries the full current. Our results are clearly in contrast with the claim that in *R. capsulatus* strains designed to enforce inter-monomer electron transfer"…electrons moved freely within and between monomers…" through a bus bar that "…distributes electrons…within the millisecond time scale of enzymatic turnover…" [18]. The similar claim in [16] to have demonstrated in *Paracoccus denitrificans* "…the previously proposed half-of-sites reactivity and inter-monomeric

electron transfer…" might seem on safer ground, because the 2-plasmid approach used could be less prone to recombination; the same might be said of the more modest claim that inter-monomer electron transfer occurs between b_L hemes with high rate and efficiency, sufficient to sustain photosynthetic growth in *R. capsulatus* [17]. However, all these claims need to be re-evaluated.

For the 1-plasmid work with which our own results can be most directly compared, Czapla et al. [61–62] revealed problems from recombination similar to those demonstrated in our work. They claimed that none of their heterodimeric strains was able to grow under anaerobic photosynthesis, but it is not clear on what experimental basis. However, all strains that could grow under these conditions had reconstructed a homodimeric wild-type complex [62], which is as we had reported. The critical experimental findings from the both groups using *R. capsulatus* [17–18] were kinetic traces showing reduction of heme b_H in the low ms range following flash excitation of the cyclic photosynthetic chain *in situ* in membrane vesicle preparations (chromatophores). Czapla et al. [61] reported a re-examination of rates, using steady-state measurements in proteins purified by affinity or ion-exchange chromatography from the different strains harboring 1-plasmid constructs. They showed that the complex from $_W$B-B^N was at least 10-fold slower than that from B-B. Their Fig. 4 showed the dependence of rate on [cyt *c*] as substrate, and complexes from all strains showed Michaelis-Menten behavior *except* $_W$B-B^N, where the rate was essentially independent of [cyt *c*]. A substantial fraction of the activity must therefore have come from some process, either non-enzymatic or of different activity, and the *bc1* complex activity was much less than the turnover of 70 s^{-1} claimed (compared to 408 s^{-1} in strain B-B). Complexes with one wild-type sequence showed about half the activity of B-B complexes, indicating both that the monomer was fully functional, and that in the homodimer, both monomers function concurrently. These activities are quite compatible with our own results, but incompatible with the claims for the bus-bar model [18]. Even if the turnover of 70 s^{-1} was applicable, the 17% of wild-type turnover would hardly justify the claim that "…Free and unregulated distribution of electrons acts like a molecular-scale bus bar…". From the data shown, the true turnover was likely <15 s^{-1}. The extensive efforts to ameliorate the recombination problem led to preparations which were relatively homogeneous, so by taking appropriate measures, the approach could offer a pathway for further characterization of heterodimeric complexes. Nevertheless, all SDS-PAGE gels of preparations isolated by ionexchange still contained significant bands at the cyt *b* monomer size, and in strain ^{N}B-B$_W$ from a construct with only 3 residues in the linker [62], this was the dominant band, and the only band labeled by anti-Strep-tag.

The brief review by Khalfaoui-Hassan et al. [63] provides a discussion of the merits of 1-plasmid and 2-plasmid approaches, and a critique of the Osyczka group's work based on the early experience of the Daldal group with a 1-plasmid system. This followed lines similar to our own. However, they also included an estimate for frequency of recombination in the range 10^{-2} when using the 1-plasmid approach, at least an order of magnitude greater than that quoted in [62].

Knowledge of the actual rates of recombination in the two systems is critical to an assessment of all other results. The pattern of band density shown by the gels in Figs. 4 and 5 suggests a high probability of recombination in the 1-plasmid system, with the reconstructed *fbcFBC* operon as the favored end-product even under non-selective conditions. However, these relative densities might be misleading. To compensate for the low copy-number of plasmid pRK415, all bands were derived by PCR amplification; by its nature, the time for synthesis of DNA dimers depends on the length of the sequence amplified, with the consequence that the shorter band could have been preferentially enhanced; other factors also come into play, making quantification difficult. Two possible

consequences should be mentioned: i) the relative intensity of bands is not necessarily in contradiction either with the reversion frequencies quoted, or with the relative homogeneity of the protein bands reported for cultures grown under non-selective conditions in [61–62]; ii) the population of heterodimeric complexes in our cultures maintaining the operon was likely substantially higher than is apparent from the band intensities after amplification of the operon DNA in Fig. 4. Consequently, we can be quite confident of our claim for expression of heterodimeric complexes that are effective if at least one monomer is active. This is in contrast to the claim in [62] that such complexes could not support photosynthetic growth.

Rates of recombination by inter- and intra-plasmid mechanisms have been studied in some detail as a function of sequence length, distance, homology, etc. [58–60, 64], from which reversion rates in the range 10^{-4} seem appropriate for the 2-plasmid approach. These should be compared to reversion rates in the 10^{-7} range seen for spontaneous point mutations. In Fig. 6 we show examples of pathways through which wild-type sequence could have been reconstructed in either plasmid, while retaining the tags. Even with frequencies in the 10^{-4} range, a simple calculation shows that cultures would be well-populated by homodimeric variants with wild-type sequence. On growth under selective conditions this population would be exponentially enhanced. The question of interest in interpretation of experimental results is therefore not whether recombination occurred, but in what fraction of the population the wild-type was reconstructed. Three points from the earlier paper [17] deserve critical attention:

i. The growth pattern in Fig. 3A of [17] is open to interpretation. It could reflect a complete failure of the heterodimeric construct to function and two different levels of reversion, or very weak growth under control of the heterodimeric construct and a more active revertant. Neither interpretation could be used to justify a significant functionality for the heterodimeric constructs.

ii. In either case, it is then necessary to reconciling these data with the kinetic data provided in Figs. 5 and 6 of [17]. These show in chromatophores containing heterodimeric complexes a rapid reduction of heme b_H on flash activation. Unbiased expression in the same cell from the two plasmids of the expression system would yield ~25 % of each of the non-functional homodimeric complexes, and maximally ~50 % heterodimeric bc_1 complex, with only one heme b_H per dimer. Since the content of cyt (c_1 + c_2), and of RC was adjusted so as to be similar, the *maximal* heme b_H reduction in the presence of antimycin expected would therefore be 25 % of that in wild-type. Of the six kinetic traces showing results from chromatophores prepared from such mixed samples, three assayed in the presence of antimycin showed an amplitude substantially greater than this (44 %, 67% and 61%). All showed halftimes similar (within the accuracy of the noise) to wildtype, and the one trace in which inhibitors were absent showed complete turnover. From other studies reported in many labs, strains with single-site mutations showing comparable bc_1 complex activity normally grow rapidly under photosynthetic conditions. These results are therefore clearly in contradiction both with the growth characteristics, and with the amplitudes expected if the kinetics reflect the activity of heterodimeric complexes. However, we note that cross-over could occur in both plasmids, so wild-type reconstructs with a full complement of heme b_H (in both monomers) might easily exceed the expected maximal amplitude, give wildtype kinetics, and account for the results.

iii. Since recombination would generate sequence changes without loss of tag (Fig. 6), neither the isolation by sequential use of tags with different affinities, nor the

labeling by tag-specific antibodies, could provide any guarantee that the sequences were those anticipated. This would also apply to the construct used in [16].

In light of the later papers [61–63], one point is unambiguously clear, that despite the steps taken to mitigate reversion, none of the above results can be used to justify the claim implicit in the earlier papers [16–18] that inter-monomer electron transfer occurs at rates compatible with an essential role in normal forward electron transfer.

Since the half-of-sites mechanism [10, 16, 32] *requires* a rate for inter-monomer electron transfer *faster* than the limiting reaction at the Q_o-site (otherwise, the two pathways for reduction of heme b_H would resolve kinetically), the evidence in support of that hypothesis now rests on Castellani et al. [16], whose results are contradicted by all others. The monotonic reduction of heme b_H in heterodimeric bc_1 complex with the same kinetics as in wild-type [16] certainly appeared to support the half-of-sites hypothesis, but that conclusion would depend absolutely on an implicit assumption that the complex expressed was that designed. This would be expected only if recombination did not occur in this system, an assumption for which we can see no justification. The reversion rates would likely be similar to those indicated in the literature [17, 58–60, 63–64], and the problems above would have to be dealt with. Since the authors did not discuss the issue, it is not possible to address the question adequately, and since details about growth conditions were not provided, it is not possible to assess the selective pressure pertaining. It is quite unlikely that reversion by recombination could have been avoided; if, as suggested by the papers cited, growth was by respiration with succinate as substrate [65], that would have provided strong selective pressure for a functional bc_1 complex.

More rigorous characterization of the *samples used experimentally* will be needed before the claims made on the basis of kinetic or spectroscopic analysis can be accepted. It would be premature to abandon the simple monomeric Q-cycle mechanism on the basis of the data reported. Our results do not exclude a functional role for inter-monomer electron transfer under some circumstances, but they do establish constraints on its scope, and raise the important question of why the reaction is so slow. If the reaction occurs, its properties *in situ* need to be established under circumstances in which no wild-type complex is expressed. We have shown in this study that the rapid kinetics seen when heterodimeric strains designed to enforce electron transfer across the dimer interface are grown photosynthetically, are due to cross-over recombination and selection for the wild-type homodimeric complex over the heterodimeric strains. Taken together with the failure to observe any evidence for inter-monomer electron transfer in the ms range in kinetic experiments using myxothiazol titrations, we conclude that inter-monomer electron transfer is not rapid enough to allow effective competition with monomeric function under conditions requiring normal turnover of the bc_1 complex, and that monomeric function remains the simplest framework for understanding the normal function.

Highlights

- Linear titration of myxothiazol inhibition is diagnostic of a monomeric mechanism
- Heterodimeric expression systems generate wild-type homodimer by recombination
- Selection for survival of functional bc_1 complex variants occurs during growth
- Intermonomer electron transfer is not competitive with monomeric turnover

Supplementary Material

Refer to Web version on PubMed Central for supplementary material.

Acknowledgments

This work was supported by a grant from NIH, NIGMS PHS 5 RO1 GM35438. We acknowledge useful discussions with Artur Osyczka, Pascal Lanciano and Bernd Ludwig at the Bioenergetics GRC, 2011, at which our results were first reported.

References

1. Baniulis D, Yamashita E, Zhang H, Hasan SS, Cramer WA. Structure-function of the cytochrome b_6f complex. Photochem. Photobiol. 2008; 84:1349–1358. [PubMed: 19067956]
2. Berry EA, Guergova-Kuras M, Huang LS, Crofts AR. Structure and function of cytochrome *bc* complexes. Annu. Rev. Biochem. 2000; 69:1005–1075. [PubMed: 10966481]
3. Crofts AR. The cytochrome bc_1 complex: function in the context of structure. Annu. Rev. Physiol. 2004; 66:689–733. [PubMed: 14977419]
4. Zhang Z, Berry EA, Huang LS, Kim SH. Mitochondrial cytochrome bc_1 complex. Subcell. Biochem. 2000; 35:541–580. [PubMed: 11192733]
5. Crofts, AR. The mechanism of ubiquinol: cytochrome *c* oxidoreductases of mitochondria and of *Rhodopseudomonas sphaeroides*. In: Martonosi, A., editor. The Enzymes of Biological Membranes. New York: Plenum; 1985. p. 347-382.
6. Crofts AR, Meinhardt SW, Jones KR, Snozzi M. The role of the quinone pool in the cyclic electron-transfer chain of *Rhodopseudomonas sphaeroides*. A modified Q-cycle mechanism. Biochim. Biophys. Acta. 1983; 723:202–218. [PubMed: 21494412]
7. Crofts AR, Shinkarev VP, Kolling DR, Hong S. The modified Q-cycle explains the apparent mismatch between the kinetics of reduction of cytochromes c_1 and b_H in the bc_1 complex. J. Biol. Chem. 2003; 278:36191–36201. [PubMed: 12829696]
8. Mitchell P. Protonmotive redox mechanism of the cytochrome b-c_1 complex in the respiratory chain: protonmotive ubiquinone cycle. FEBS Lett. 1975; 56:1–6. [PubMed: 239860]
9. Mitchell P. Possible molecular mechanisms of the protonmotive function of cytochrome systems. J. Theor. Biol. 1976; 62:327–367. [PubMed: 186667]
10. Covián R, Trumpower BL. Rapid electron transfer between monomers when the cytochrome bc_1 complex dimer is reduced through center N. J. Biol. Chem. 2005; 280:22732–22740. [PubMed: 15833742]
11. Crofts AR. The Q-cycle - A Personal Perspective. Photosynth. Res. 2004; 80:223–243. [PubMed: 16328823]
12. Crofts AR, Holland JT, Victoria D, Kolling DR, Dikanov SA, Gilbreth R, Lhee S, Kuras R, Kuras MG. The Q-cycle reviewed: How well does a monomeric mechanism of the bc_1 complex account for the function of a dimeric complex?, Biochim. Biophys. Acta. 2008; 1777:1001–1019. [PubMed: 18501698]
13. Gong X, Yu L, Xia D, Yu CA. Evidence for electron equilibrium between the two hemes b_L in the dimeric cytochrome bc_1 complex. J. Biol. Chem. 2005; 280:9251–9257. [PubMed: 15615714]
14. Osyczka A, Moser CC, Daldal F, Dutton PL. Reversible redox energy coupling in electron transfer chains. Nature. 2004; 427:607–612. [PubMed: 14961113]
15. Shinkarev VP, Wraight CA. Intermonomer electron transfer in the bc_1 complex dimer is controlled by the energized state and by impaired electron transfer between low and high potential hemes. FEBS Lett. 2007; 581:1535–1541. [PubMed: 17399709]
16. Castellani M, Covian R, Kleinschroth T, Anderka O, Ludwig B, Trumpower BL. Direct demonstration of half-of-the-sites reactivity in the dimeric cytochrome bc_1 complex: enzyme with one inactive monomer is fully active but unable to activate the second ubiquinol oxidation site in response to ligand binding at the ubiquinone reduction site. J. Biol. Chem. 2010; 285:502–510. [PubMed: 19892700]

17. Lanciano P, Lee DW, Yang H, Darrouzet E, Daldal F. Intermonomer electron transfer between the low-potential *b* hemes of cytochrome *bc*. Biochemistry. 2011; 50:1651–1663. [PubMed: 21261281]
18. Swierczek M, Cieluch E, Sarewicz M, Borek A, Moser CC, Dutton PL, Osyczka A. An electronic bus bar lies in the core of cytochrome bc_1. Science. 2010; 329:451–454. [PubMed: 20651150]
19. Covián R, Gutierrez-Cirlos EB, Trumpower BL. Anti-cooperative oxidation of ubiquinol by the yeast cytochrome bc_1 complex. J. Biol. Chem. 2004; 279:15040–15049. [PubMed: 14761953]
20. Covián R, Trumpower BL. Regulatory interactions in the dimeric cytochrome bc_1 complex: The advantages of being a twin. Biochim. Biophys. Acta. 2008; 1777:1079–1091. [PubMed: 18471987]
21. Covián R, Trumpower BL. The rate-limiting step in the cytochrome bc_1 complex is not changed by inhibition of cytochrome *b*-dependent deprotonation: implications for the mechanism of ubiquinol oxidation at center P of the bc_1 complex. J. Biol. Chem. 2009; 284:14359–14367. [PubMed: 19325183]
22. Guergova-Kuras M, Salcedo-Hernandez R, Bechmann G, Kuras R, Gennis RB, Crofts AR. Expression and one-step purification of a fully active polyhistidine-tagged cytochrome bc_1 complex from *Rhodobacter sphaeroides*. Protein Expr. Purif. 1999; 15:370–380. [PubMed: 10092497]
23. Kuras R, Guergova-Kuras M, Crofts AR. Steps toward constructing a cytochrome b_6f complex in the purple bacterium *Rhodobacter sphaeroides*: an example of the structural plasticity of a membrane cytochrome. Biochemistry. 1998; 37:16280–16288. [PubMed: 9819220]
24. Yun C-H, Beci R, Crofts AR, Kaplan S, Gennis RB. Cloning and DNA sequencing of the *fbc* operon encoding the cytochrome bc_1 complex from *Rhodobacter sphaeroides*: Characterization of *fbc* deletion mutants, and complementation by a site-specific mutational variant. Eur. J. Biochem. 1990; 194:399–411. [PubMed: 2176595]
25. Bowyer JR, Tierney GV, Crofts AR. Secondary electron transfer in chromatophores of *Rhodopseudomonas capsulata* A1a pho^+. Binary out-of-phase oscillations in ubisemiquinone formation and cytochrome b_{50} reduction with consecutive light flashes. FEBS Lett. 1979; 101:201–206. [PubMed: 446736]
26. Bechmann G, Weiss H, Rich P. Nonlinear inhibition curves for tight-binding inhibitors of dimeric ubiquinol-cytochrome *c* oxidoreductase - evidence for rapid inhibitor mobility. Eur. J. Biochem. 1992; 208:315–325. [PubMed: 1325904]
27. Fernandez-Velasco J, Crofts AR. Complexes or super complexes: Inhibitor titrations show that electron transfer in chromatophores from *Rhodobacter sphaeroides* involves a dimeric ubiquinol: cytochrome c_2 oxidoreductase, and is delocalized. Biochem. Soc. Trans. 1991; 19:588–593. [PubMed: 1664388]
28. Tsai A-L, Kauten R, Palmer G. The interaction of yeast complex III with some respiratory inhibitors. Biochim. Biophys. Acta. 1985; 806:418–426. [PubMed: 2982396]
29. Meinhardt SW, Crofts AR. The role of cytochrome *b*-566 in the electron-transfer chain of *Rhodopseudomonas sphaeroides*. Biochim. Biophys. Acta. 1983; 723:219–230.
30. Yun CH, Crofts AR, Gennis RB. Assignment of the histidine axial ligands to the cytochrome b_H and cytochrome b_L components of the bc_1 complex from *Rhodobacter sphaeroides* by site-directed mutagenesis. Biochemistry. 1991; 30:6747–6754. [PubMed: 1648391]
31. Meinhardt SW, Crofts AR. Kinetic and thermodynamic resolution of cytochrome c_1 and cytochrome c_2 from *Rhodopseudomonas sphaeroides*. FEBS Lett. 1982; 149:223–227.
32. Trumpower BL. A concerted, alternating sites mechanism of ubiquinol oxidation by the dimeric cytochrome bc_1 complex. Biochim. Biophys. Acta. 2002; 1555:166–173. [PubMed: 12206910]
33. Balabin IA, Onuchic JN. Dynamically controlled protein tunneling paths in photosynthetic reaction centers. Science. 2000; 290:114–117. [PubMed: 11021791]
34. DeVault D. Quantum mechanical tunnelling in biological systems. Q. Rev. Biophys. 1980; 13:387–564. [PubMed: 7015406]
35. Kuki A, Wolynes PG. Electron tunneling paths in proteins. Science. 1987; 236:1647–1652. [PubMed: 3603005]

36. Marcus RA, Sutin N. Electron transfers in chemistry and biology. Biochim. Biophys. Acta. 1985; 811:265–322.
37. Nishioka H, Kimura A, Yamato T, Kawatsu T, Kakitani T. Interference, fluctuation, and alternation of electron tunneling in protein media. 1. Two tunneling routes in photosynthetic reaction center alternate due to thermal fluctuation of protein conformation. J. Phys. Chem. B. 2005; 109:1978–1987. [PubMed: 16851182]
38. Onuchic JN, Beratan DN. A predictive theoretical model for electron tunneling pathways in proteins. J. Chem. Phys. 1990; 92:722–733.
39. Prytkova TR, Kurnikov IV, Beratan DN. Coupling coherence distinguishes structure sensitivity in protein electron transfer. Science. 2007; 315:622–625. [PubMed: 17272715]
40. Gray HB, Winkler JR. Long-range electron transfer. Proc. Natl. Acad. Sci. U. S. A. 2005; 102:3534–3539. [PubMed: 15738403]
41. Moser CC, Dutton PL. Engineering protein structure for electron transfer function in photosynthetic reaction centers. Biochim. Biophys. Acta. 1992; 1101:171–176. [PubMed: 1633183]
42. Moser CC, Farid TA, Chobot SE, Dutton PL. Electron tunnelling chains of mitochondria. Biochim. Biophys. Acta. 2006; 1757:1096–1109. [PubMed: 16780790]
43. Moser CC, Page CC, Chen XX, Dutton PL. Biological electron tunnelling through protein media. J. Biol. Inorg. Chem. 1997; 2:393–398.
44. Noy D, Moser CC, Dutton PL. Darwin at the molecular scale: selection and variance in electron tunnelling proteins including cytochrome *c* oxidase. Biochim. Biophys. Acta. 2006; 1757:90–106. [PubMed: 16457774]
45. Page CC, Moser CC, Chen X, Dutton PL. Natural engineering principles of electron tunnelling in biological oxidation-reduction. Nature. 1999; 402:47–52. [PubMed: 10573417]
46. Hopfield JJ. Electron transfer between biological molecules by thermally activated tunneling. Proc. Natl. Acad. Sci. U. S. A. 1974; 71:3640–3644. [PubMed: 16592178]
47. Moser CC, Anderson JL, Dutton PL. Guidelines for tunneling in enzymes. Biochim. Biophys. Acta. 2010; 1797:1573–1586. [PubMed: 20460101]
48. Crofts AR, Rose S. Marcus treatment of endergonic reactions: a commentary. Biochim. Biophys. Acta. 2007; 1767:1228–1232. [PubMed: 17720135]
49. Winkler JR, Di Bilio AJ, Farrow NA, Richards JH, Gray HB. Electron tunneling in biological molecules. Pure Appl. Chem. 1999; 71:1753–1764.
50. Hoffman BM, Celis LM, Cull DA, Patel AD, Seifert JL, Wheeler KE, Wang J, Yao J, Kurnikov I, Nocek JM. Differential influence of dynamic processes on forward and reverse electron transfer across a protein-protein interface. Proc. Natl. Acad. Sci. U. S. A. 2005; 102:3564–3569. [PubMed: 15738411]
51. Walker FA. Magnetic spectroscopic (EPR, ESEEM, Mössbauer, MCD and NMR) studies of low-spin ferriheme centers and their corresponding heme proteins. Coord. Chem. Rev. 1999; 185–186:471–534.
52. Walker FA. Models of the bis-histidine-ligated electron-transferring cytochromes. Comparative geometric and electronic structure of low-spin ferro- and ferrihemes. Chem. Rev. 2004; 104:589–615. [PubMed: 14871136]
53. San Filippo J, Sung P, Klein H. Mechanism of eukaryotic homologous recombination. Annu Rev Biochem. 2008; 77:229–257. [PubMed: 18275380]
54. Smith GR. Homologous recombination in procaryotes. Microbiol. Rev. 1988; 52:1–28. [PubMed: 3280962]
55. Simon R, Priefer U, Pühler A. A broad host range mobilization system for in vivo genetic engineering: transposon mutagenesis in Gram negative bacteria. Bio/technology. 1983; 1:784–791.
56. Taylor RG, Walker DC, McInnes RR. *E. coli* host strains significantly affect the quality of small scale plasmid DNA preparations used for sequencing. Nucleic Acids Res. 1993; 21:1677–1678. [PubMed: 8479929]
57. Bi X, Liu LF. *recA*-independent and *recA*-dependent intramolecular plasmid recombination. Differential homology requirement and distance effect. J. Mol. Biol. 1994; 235:414–423. [PubMed: 8289271]

58. Bi X, Liu LF. *recA*-independent DNA recombination between repetitive sequences: mechanisms and implications. Prog. Nucleic Acid Res. Mol. Biol. 1996; 54:253–292. [PubMed: 8768077]
59. Lovett ST, Drapkin PT, Sutera VA Jr, Gluckman-Peskind TJ. A sister-strand exchange mechanism for *recA*-independent deletion of repeated DNA sequences in *Escherichia coli*. Genetics. 1993; 135:631–642. [PubMed: 8293969]
60. Lovett ST, Hurley RL, Sutera VA Jr, Aubuchon RH, Lebedeva MA. Crossing over between regions of limited homology in *Escherichia coli*. RecA-dependent and RecA-independent pathways. Genetics. 2002; 160:851–859. [PubMed: 11901106]
61. Czapla M, Borek A, Sarewicz M, Osyczka A. Enzymatic activities of isolated cytochrome bc_1-like complexes containing fused cytochrome *b* subunits with asymmetrically inactivated segments of electron transfer chains. Biochemistry. 2012; 51:829–835. [PubMed: 22233445]
62. Czapla M, Borek A, Sarewicz M, Osyczka A. Fusing two cytochromes *b* of *Rhodobacter capsulatus* cytochrome bc_1 using various linkers defines a set of protein templates for asymmetric mutagenesis. Protein Eng. Des. Sel. 2012; 25:15–25. [PubMed: 22119789]
63. Khalfaoui-Hassani B, Lanciano P, Lee DW, Darrouzet E, Daldal F. Recent advances in cytochrome bc_1: Inter monomer electronic communication? FEBS Lett. 2011; 586:617–621. [PubMed: 21878327]
64. Chedin F, Dervyn E, Dervyn R, Ehrlich SD, Noirot P. Frequency of deletion formation decreases exponentially with distance between short direct repeats. Mol. Microbiol. 1994; 12:561–569. [PubMed: 7934879]
65. Ludwig B. Cytochrome *c* oxidase from *Paracoccus denitrificans*. Methods Enzymol. 1986; 126:153–159. [PubMed: 2856122]
66. Esser L, Elberry M, Zhou F, Yu CA, Yu L, Xia D. Inhibitor-complexed structures of the cytochrome bc_1 from the photosynthetic bacterium *Rhodobacter sphaeroides*. J. Biol. Chem. 2008; 283:2846–2857. [PubMed: 18039651]
67. Moser CC, Page CC, Farid R, Dutton PL. Biological electron transfer. J. Bioenerg. Biomembr. 1995; 27:263–274. [PubMed: 8847340]

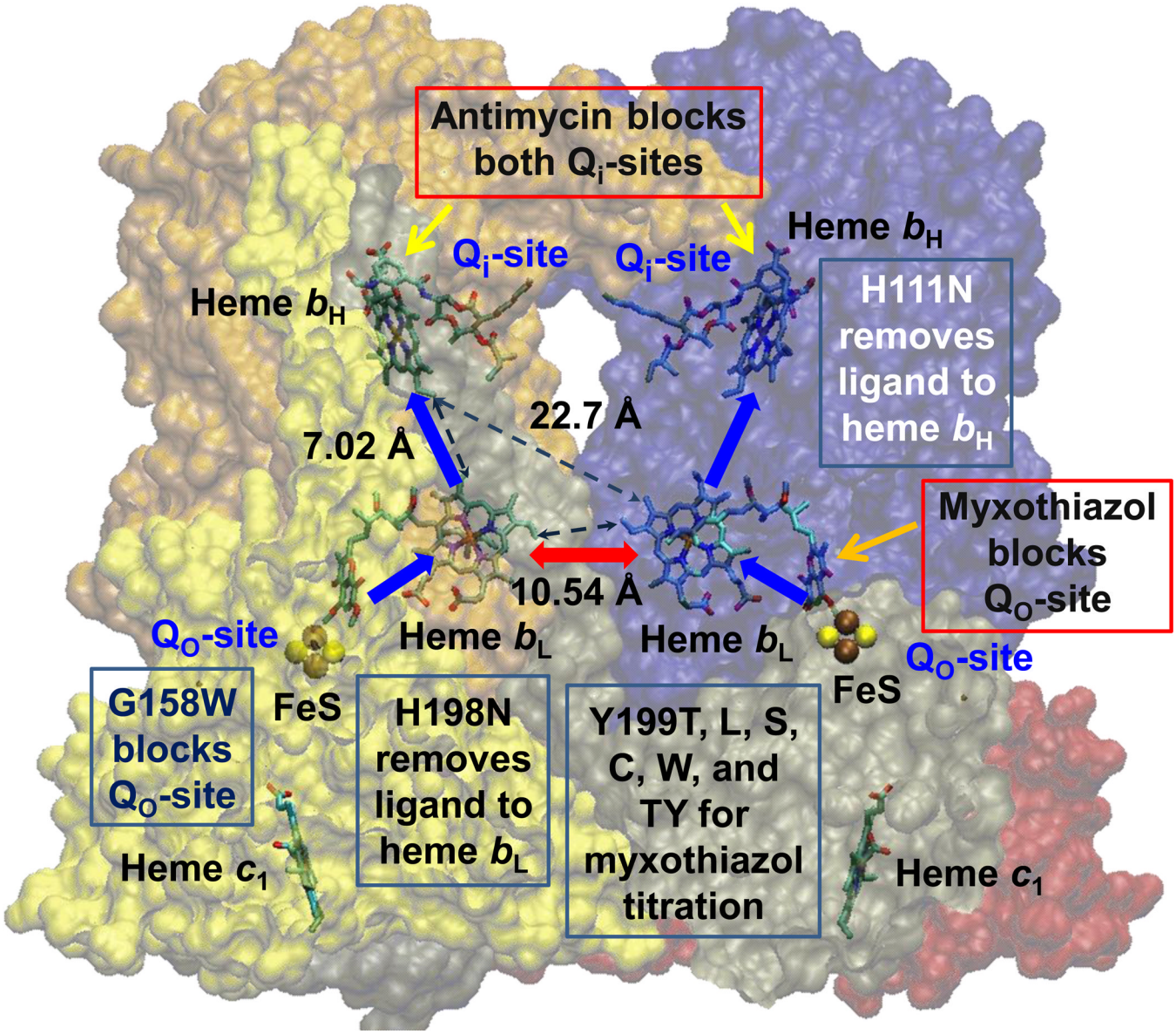

Fig. 1. Scheme to show rationale for the study of inter-monomer electron transfer

With both Q_i-sites blocked by antimycin, electrons cannot exit from heme b_H. If one monomer is blocked by myxothiazol at the Q_o-site, the unblocked Q_o-site would deliver electrons to both monomers if inter-monomer electron transfer could occur rapidly between the b_L hemes (red arrow). Blue arrows show monomeric electron transfer. Mutations used to block different partial process were G158W (Q_o-site), H111N (heme b_H), and H198N (heme b_L). See also Table 2 and Fig S1. Structure is from PDB 2QJY [66], in which occupancy by stigmatellin defines the Q_o-site, and occupancy by ubiquinone-10 defines the Q_i-site.

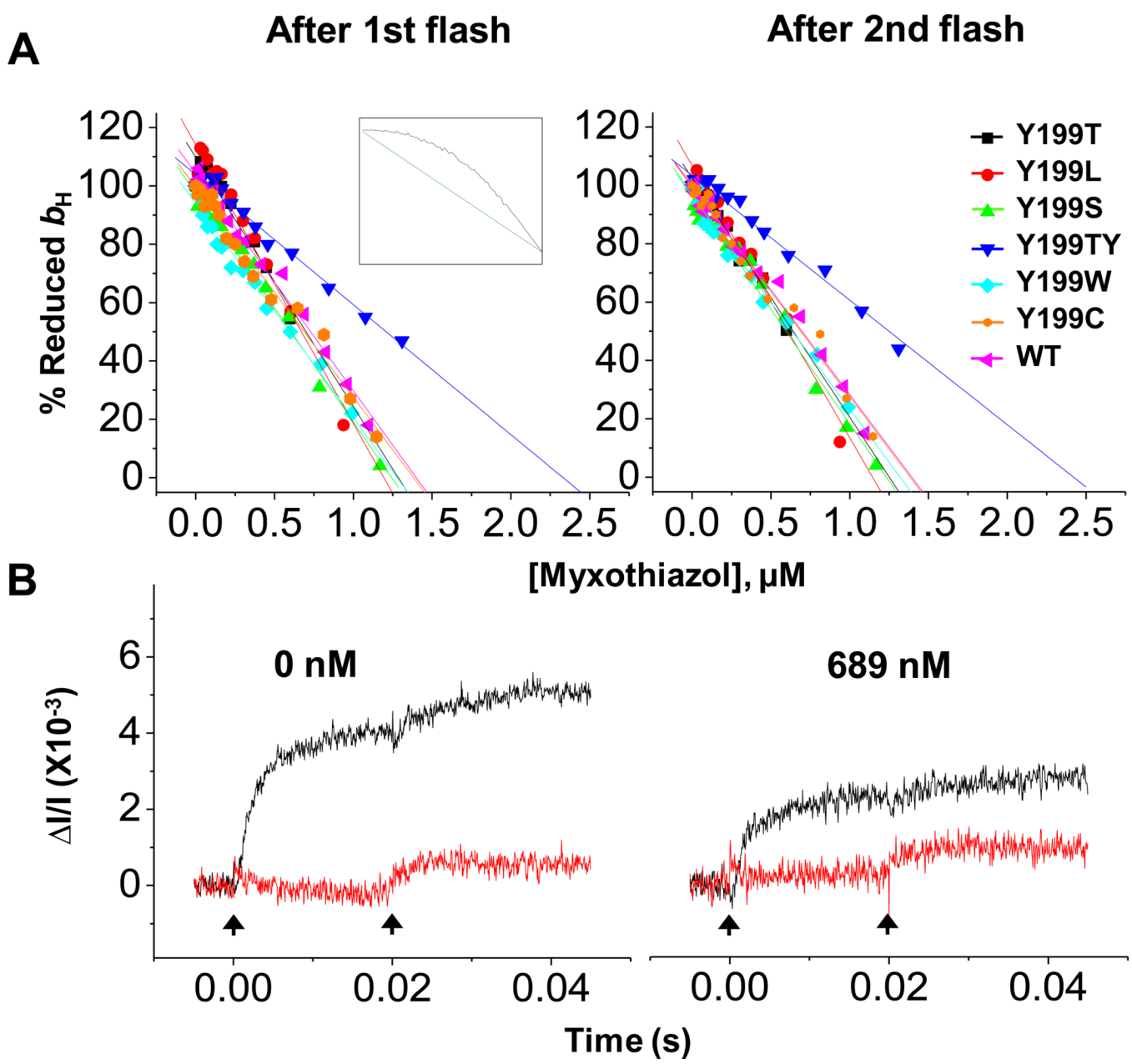

Fig. 2. Titrations of Q_o-site with myxothiazol

(A) Fraction (% of change with no inhibitor) of reduced b_H at 20 ms (after 1st flash) and 50 ms (after 2nd flash) versus inhibitor concentration. Chromatophores from native and mutant strains of *R. sphaeroides* were poised at E_h 100 ±10 mV at pH 7.0 and 20 °C. Rates were measured in the presence of antimycin to block oxidation of heme b_H through the Q_i-site, as Q_o-sites were titrated with myxothiazol. Insert shows titration curves expected without (straight line, green) or with (convex curve, black) inter-monomer electron transfer, from simulation (see [26]). **(B)** Kinetics of reduction of heme b_H (black) and heme b_L (red) in wild-type following two flashes. Myxothiazol was added at the concentrations shown. The vertical arrows indicate flash activation. The pattern is diagnostic of monomeric function.

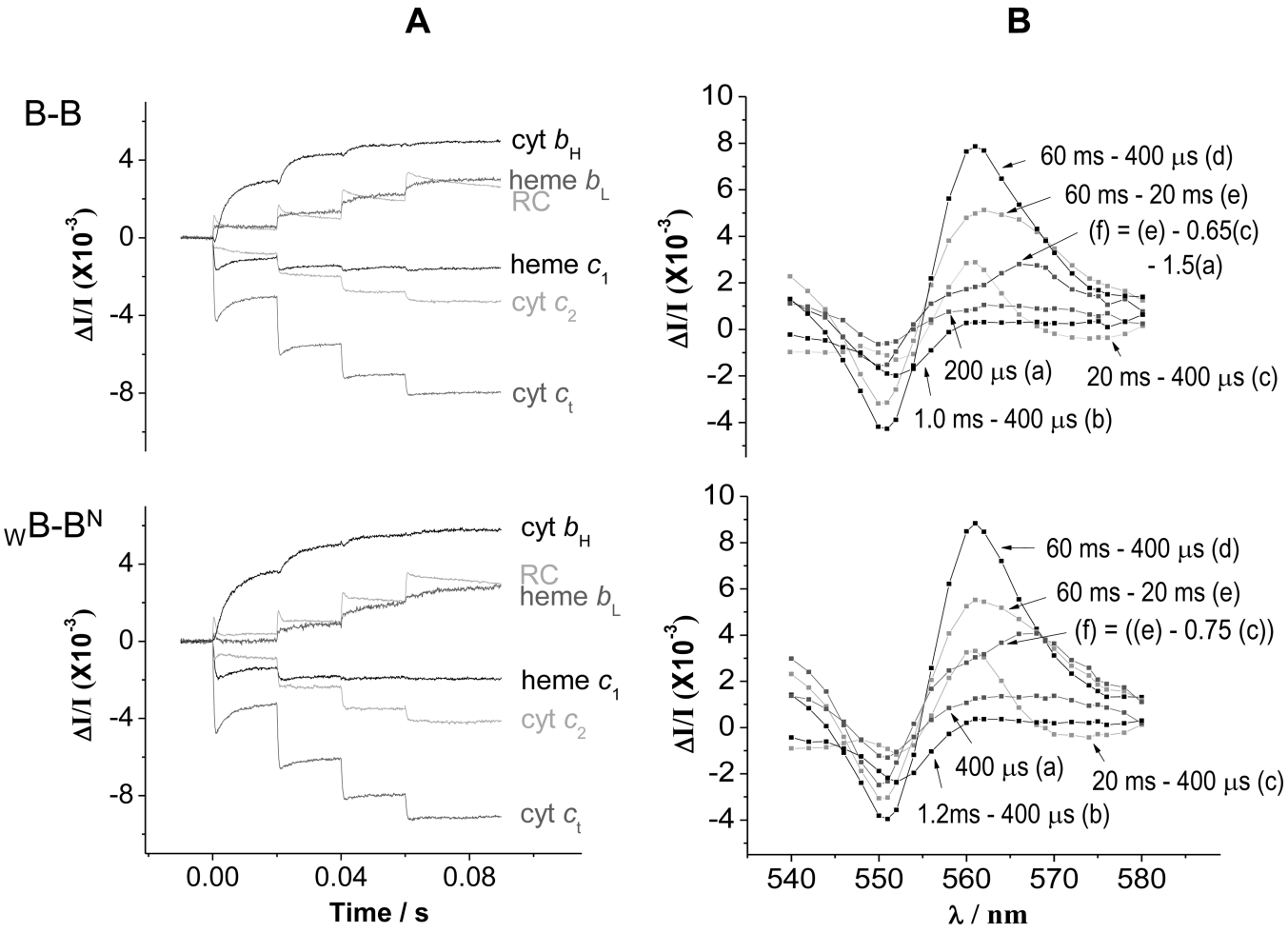

Fig. 3. Kinetics in strains containing heterodimeric constructs

(A) Kinetic traces for the components of the photosynthetic chain, measured from difference kinetics at the following wavelengths. Reaction center (RC); 542 nm; cyt c_t, 551-542 nm; cyt c_2, 550–554 nm; heme c_1, 552-548 nm; heme b_H, 561–569 nm; heme b_L, (566–575 nm) – 0.5(heme b_H) (with additional small corrections for *c*-type hemes and RC. **(B)** Spectra at selected times showing involvement of hemes b_H, b_L, c_1, c_2, and RC. (a) Change 400 μs after first flash shows mainly cyt c_2 oxidation; (b) over the period 0.4–1.2 ms, heme c_1 oxidation dominates the change; (c) from 0.4 to 20 ms, heme b_H reduction dominates the kinetics, with a derivative spectrum in the range 548–554 nm showing electron transfer from heme c_1 to cyt c_2; (d) the changes after the second and subsequent flashes contain contributions from all centers; (e) after the second flash, heme b_L and most of the remaining heme b_H go reduced; (f) subtraction of a fraction of the change (c) reveals the spectrum of heme b_L reduction. RC changes contribute through a rather flat spectrum across this wavelength span, but dominate at 542 nm, where the heme changes are approximately isosbestic. Times given are after flash 1 at 0 s. Flashes are spaced 20 ms apart. Chromatophores from B-B and $_W$B-B^N cells were poised at E_h ~120 mV by addition of 2 mM ascorbate, with 2 mM KCN added to inhibit cyt oxidase activity.

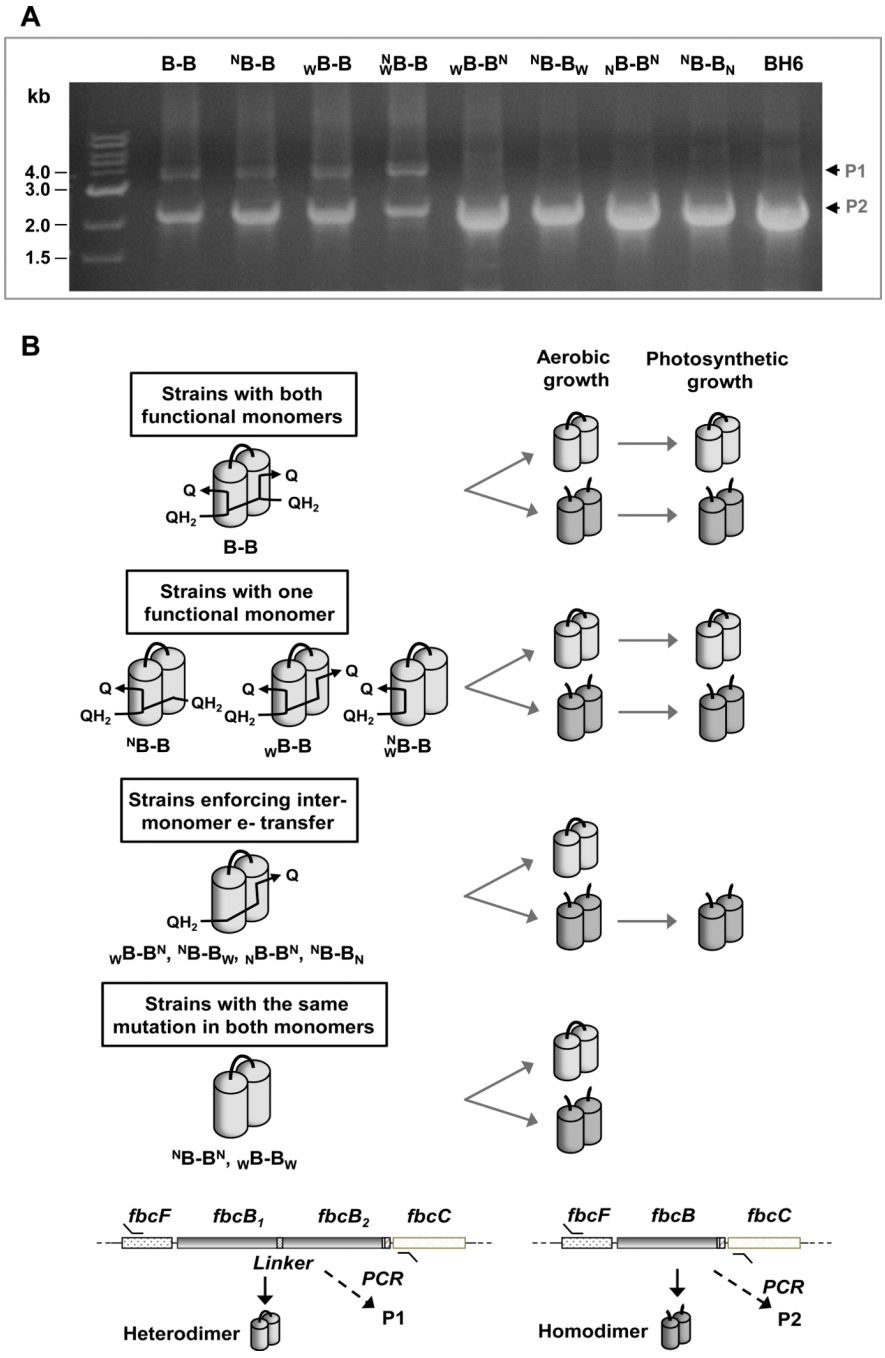

Fig. 4. Selection of functional bc_1 complex variants for survival during growth

(A) Constructs of *fbc* operon maintained at high abundance during photosynthetic growth. The bands represent PCR products amplified from photosynthetic cultures used in kinetic analysis. Both the heterodimeric construct (P1) and the recombinant homodimeric re-construct (P2) were maintained at high abundance in all strains with at least one functional monomer. On the other hand, in the strains which contained a mutation crippling monomeric function to enforce inter-monomer electron transfer, only the recombinant construct for the wild-type homodimer (P2) was maintained in the culture. The PCR bands from BH6 strain which contains a 6xHis-tagged homodimeric construct, was used as a control size marker.

(B) Schematic representation of the selection of constructs coding for functional bc_1 complex. The cultures of *R. sphaeroides* retain only the constructs expressing functional bc_1 complex when bc_1 complex is required for survival under anaerobic photosynthetic condition.

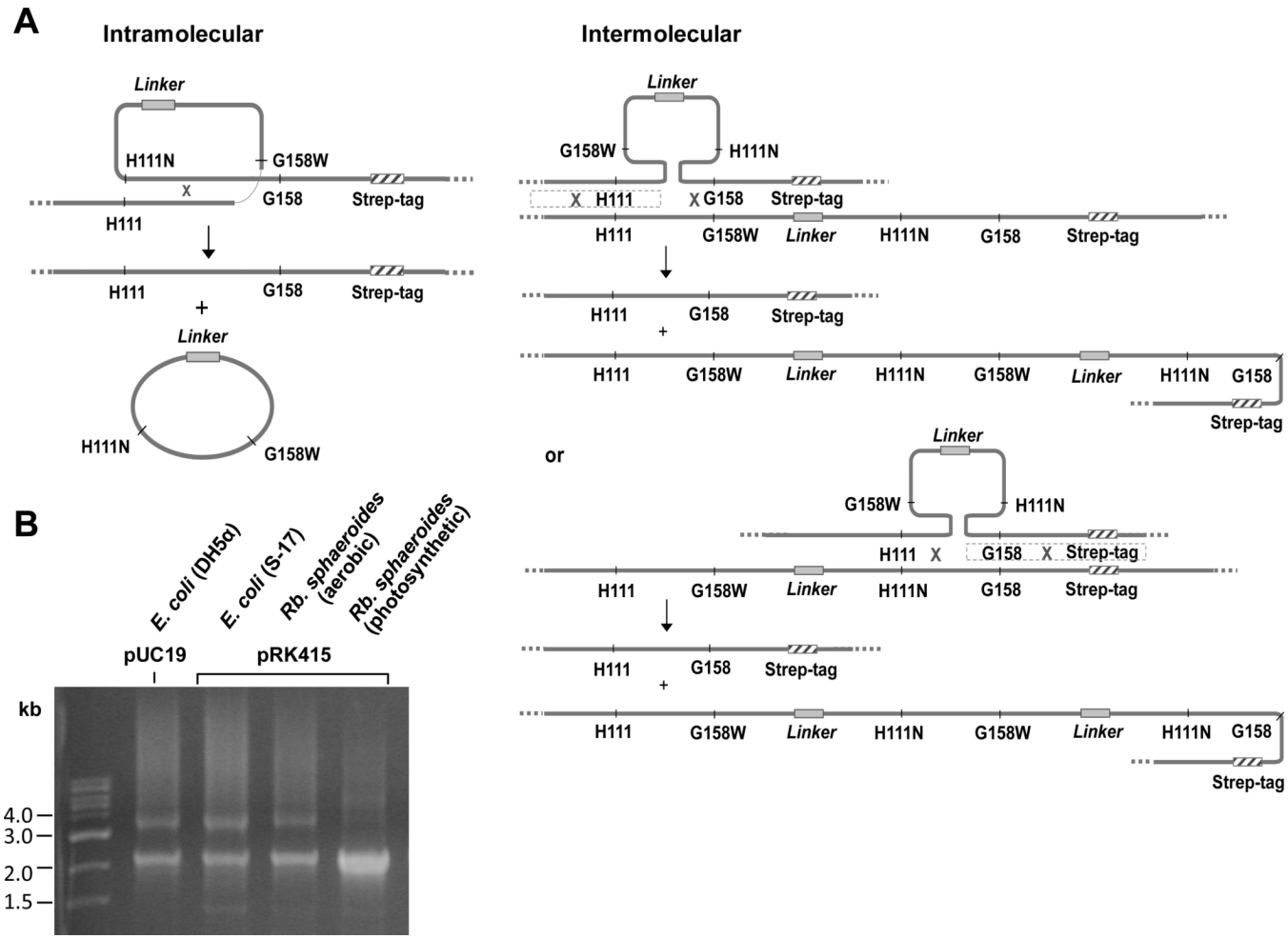

Fig. 5. Generation of wild-type homodimer by homologous recombination in 1-plasmid approach

(A) Schematic showing the generation of recombinant construct for homodimer from heterodimeric construct. When two genes with substantially the same sequence are present in the cell, cross-over (x marks) occurs by homologous recombination within a plasmid or between plasmids, shown here by the example of $_{W}$B-B^{N}. **(B)** Constructs retained at different stages of $_{W}$B-B^{N} heterodimeric construct. Only recombinant homodimeric construct with wild-type sequence remained at a significant level when grown photosynthetically. All the PCR products in the major bands contained coding for the strep-tag.

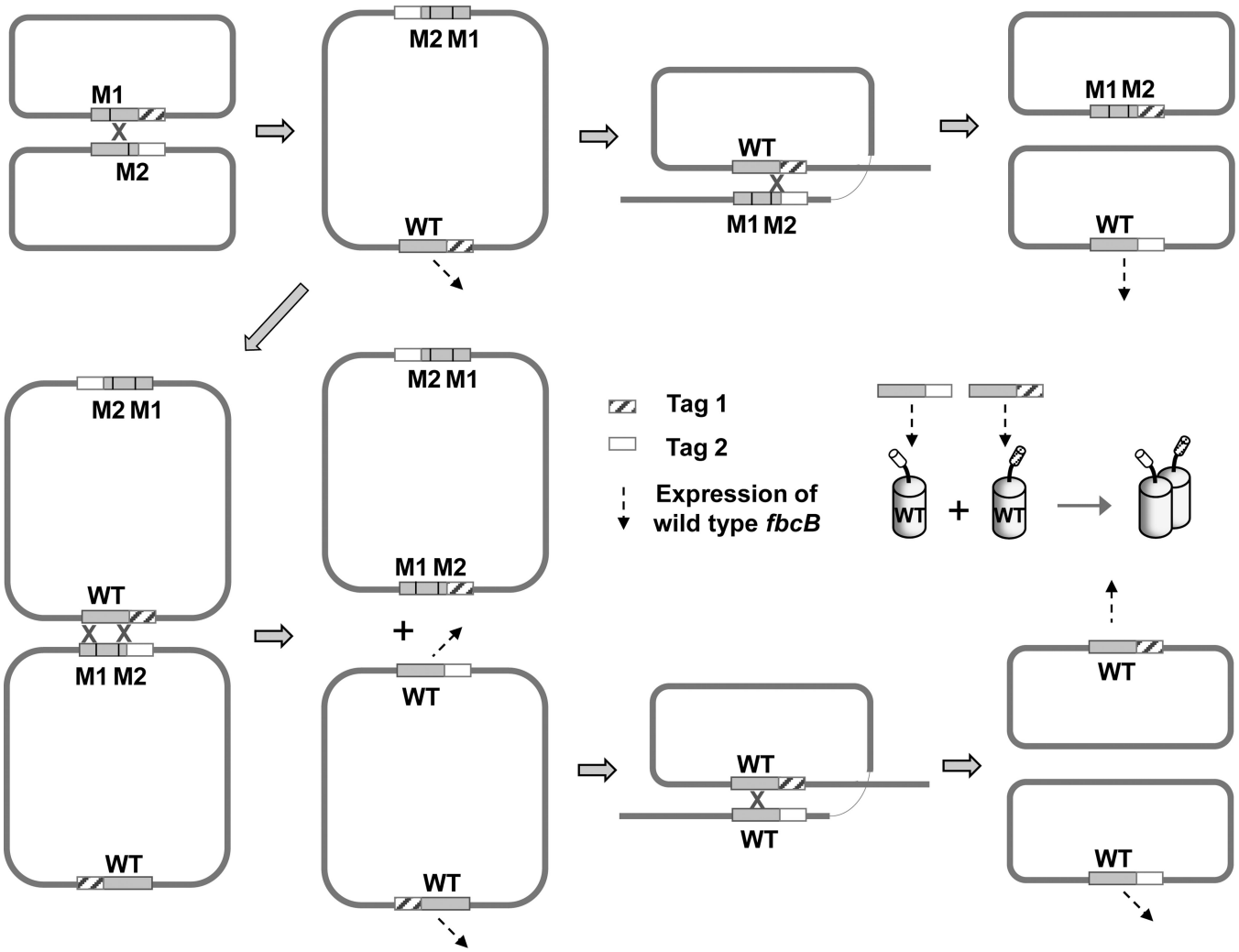

Fig. 6. Representative cross-over events generating wild type *fbcB* in 2-plasmid approach

Single cross-over between two different plasmids containing mutant *fbc* operons with different mutations in *fbcB*, generates a dimeric integrant plasmid, and another round of single cross-over recombination allows production of wild-type sequences of *fbcB* with two different tags. Double cross-over recombination between the two different plasmids and between dimeric integrant plasmids also generates wild type *fbcB* sequences containing two different tags. M1 and M2 denote different mutation sites in *fbcB*.

Table 1

Rate constants expected from structures and a Moser-Dutton treatment of distance dependence.

heme *b* pairs involved and parameters assumed	**Marcus-Moser-Dutton (k_{cat}/s^{-1})**
b_L-b_H through 2-vinyl (ΔG° = −60 mV, λ = 0.75 V, R = 7.02 Å)	1.73×10^8
b_L-b_H through 2-vinyl (ΔG° = −130 mV, λ = 0.75 V, R = 7.02 Å)	5.68×10^8
b_L-b_L through 4-vinyl (ΔG° = −0 mV, λ = 0.75 V, R = 10.54 Å)	4.08×10^5
b_L-b_L through 4-vinyl (ΔG° = −60 mV, λ = 0.75 V, R = 10.54 Å)	1.25×10^6

Notes. Rate constants were calculated using the following equation:

$$\log_{10} k_{cat} = 13 - \frac{\beta}{2.303}(R - 3.6) - \gamma\left(\frac{(\Delta G^o + \lambda)^2}{\lambda}\right)$$

Values used for other parameters were β = 1.4, γ = 4.23. We have avoided use of the Hopfield approximation suggested earlier [67] through use of modifier, γ = 3.1, of the activation-energy term since it causes loss of detailed balance in consideration of forward and reverse rate constants [12, 48].

Table 2

Heterodimeric strains and their growth properties.

Strain	Genotype		Growth properties	
	fbcB$_1$	*fbcB*$_2$	*aerobic*	*photosynthetic*
B-B	Wild type	Wild type	+	+
^{N}B-B	H111N	Wild type	+	+
$_{W}$B-B	G158W	Wild type	+	+
$^{N}_{W}$**B–B**	H111N/G158W	Wild type	+	+
B–B$^{N}_{W}$	Wild type	H111N/G158W	+	+
$_{W}$B-B^{N}	G158W	H111N	+	+
^{N}B-B$_{W}$	H111N	G158W	+	+
$^{N}_{N}$**B–B**	H111N/H198N	Wild type	+	+
B–B$^{N}_{N}$	Wild type	H111N/H198N	+	+
$_{N}$B-B^{N}	H198N	H111N	+	+
^{N}B-B$_{N}$	H111N	H198N	+	+
^{N}B-B^{N}	H111N	H111N	+	−
$_{W}$B-B$_{W}$	G158W	G158W	+	−